

ChemComm

Accepted Manuscript



This is an *Accepted Manuscript*, which has been through the Royal Society of Chemistry peer review process and has been accepted for publication.

Accepted Manuscripts are published online shortly after acceptance, before technical editing, formatting and proof reading. Using this free service, authors can make their results available to the community, in citable form, before we publish the edited article. We will replace this *Accepted Manuscript* with the edited and formatted *Advance Article* as soon as it is available.

You can find more information about *Accepted Manuscripts* in the [Information for Authors](#).

Please note that technical editing may introduce minor changes to the text and/or graphics, which may alter content. The journal's standard [Terms & Conditions](#) and the [Ethical guidelines](#) still apply. In no event shall the Royal Society of Chemistry be held responsible for any errors or omissions in this *Accepted Manuscript* or any consequences arising from the use of any information it contains.

COMMUNICATION

Asymmetrical Squaraines for High-Performance Small-Molecule Organic Solar Cells with Short Circuit Current of over 12 mA cm^{-2} †

Cite this: DOI: 10.1039/x0xx00000x

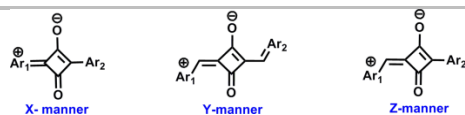
Received 00th January 2012,
Accepted 00th January 2012Yao Chen,‡^a Youqin Zhu,‡^b Daobin Yang,^a Qian Luo,^a Lin Yang,^a Yan Huang,^{*a}
Suling Zhao^{*b} and Zhiyun Lu^{*a}

DOI: 10.1039/x0xx00000x

www.rsc.org/

An asymmetrical squaraine dye (Py-3) with its two electron-donating aryls directly linked to the electron withdrawing squaric acid core possesses an ideal bandgap of 1.33 eV together with an intense and broad absorption band in 550–950 nm, hence the solution-processed solar cells display an impressive J_{sc} of 12.03 mA cm^{-2} and PCE of 4.35%.

Owing to their intense absorption in Vis-NIR regions and good photochemical/photophysical stability, squaraine dyes have drawn much attention in small-molecule organic solar cell (SMOSC) applications.¹ According to molecular framework, photovoltaic squaraine (SQ) dyes are generally classified into symmetrical (D-A-D, SSQ) and asymmetrical (D-A-D', ASQ) ones, in which squaric acid core acts as the electron acceptor (A) subunit, and electron-rich aromatic systems act as the electron donor (D or D') subunits. In addition, as illustrated in Scheme 1, for SSQ dyes, their D aryls could be linked to the A unit through either X-manner^{1a, 1c} (D aryls are connected to A subunit directly) or Y-manner² (D aryls are linked to A subunit via methylylidene bridges); while for ASQ dyes, their D and D' aryls could be



Scheme 1 Typical molecular frameworks of photovoltaic squaraine dyes.

^a Key Laboratory of Green Chemistry and Technology (Ministry of Education), College of Chemistry, Sichuan University, Chengdu 610064, P. R. China. E-mail: huangyan@scu.edu.cn, luzhiyun@scu.edu.cn

^b Key Laboratory of Luminescence and Optical Information (Ministry of Education), Institute of Optoelectronics Technology, Beijing Jiaotong University, Beijing 100044, P. R. China. Email: slzhao@bjtu.edu.cn

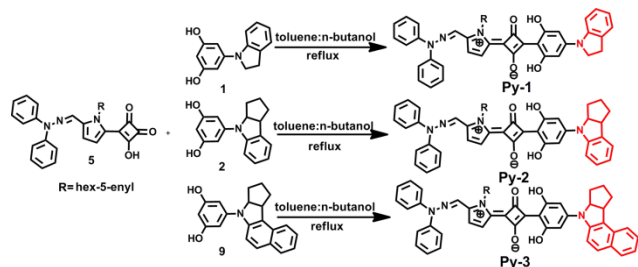
† Electronic supplementary information (ESI) available: Synthetic procedure, CV curves, charge carrier mobility measurement results and AFM images. For ESI and other electronic format see DOI:

‡ The first two authors contributed equally to this work.

linked to A subunit not only through X- and Y-manners, but also through an extra Z-manner,³ in which D and D' segments are connected to A subunit directly and *via* a methylylidene bridge, respectively.⁴

Thanks to the recent enthusiastic research efforts, high-performance SSQ-based SMOSCs with record power conversion efficiency (PCE) of 5.50%⁵ for X-manner and 3.14%^{2a} for Y-manner have been achieved, whereas, ASQ-based SMOSCs just showed relative poor performance, with maximum PCE of 2.05% and 1.22% for Y- and Z-manner,⁶ respectively. Therefore, ASQs have been considered as futureless organic photovoltaic (OPV) materials for a long time, and have received little research attention. However, in comparison with ASQs bearing a D-A-D' molecular skeleton, D-A-D-structured SSQs should possess less plenty room for molecular tailoring due to the lack of diverse combination ways of D and D' subunits as well as the Z-mannered molecular skeleton. Recently, through delicate molecular design, we have developed some high performance OPV ASQs *via* Z-manner. SMOSCs using them as electron donor materials could show maximum open circuit voltage (V_{oc}) of 1.12 V, short circuit current (J_{sc}) of 11.03 mA cm^{-2} , and PCE of 4.29%^{1e, 7}, indicating that ASQs are also promising OPV materials.

It became clear from the studies of Claudia Gude *et al.* that the photophysical properties in squaraine compounds correlate highly with their connected manners,⁸ while all the hitherto developed OPV ASQs have been construction through either Y- or Z-manner, and no X-mannered examples have been exploited,^{1, 2} herein, we designed and synthesized a series of novel ASQ dyes (**Py-1~3**, molecular structure shown in Scheme 2) whose D and D' segments are linked to the A subunit *via* X-manner. Through rational molecular design, one of the objective compound **Py-3** could show an ideal bandgap of 1.33 eV together with an intense and broad absorption band in 550–950 nm, and SMOSC using **Py-3** as electron donor could display an excellent J_{sc} of 12.03 mA cm^{-2} and a high PCE of 4.35%, which are the highest J_{sc} and PCE among all the reported ASQ-based SMOSCs,^{1e} indicating ASQs bearing X-mannered molecular framework are quite perspective OPV materials. Since most squaraine dyes suffer from narrow absorption band, which is adverse to the light-harvesting process in solar cells,^{1c, 1e} we aimed at the exploitation of ASQs showing relatively broad



Scheme 2 Molecular structure and synthetic route of the target molecules **Py-1**~**3**.

absorption spectra in the Vis-NIR region. Inspired by the discovery of Marks^{1a, 1b} *et al* that squaraines containing (*E*)-2-((2,2-diphenylhydrazono)-methyl)-1-(hex-5-enyl)-1*H*-pyrrole D unit own relatively broad absorption bands and good hole mobility due to the presence of double-bond end-capped alkyl side-chains, and our finding that *N*-(3,5-dihydroxyphenyl)indoline with planar geometry is an ideal D' segment for constructing high performance OPV ASQs with relatively low bandgap, initially, we designed and synthesized compound **Py-1** with (*E*)-2-((2,2-diphenylhydrazono) methyl)-1-(hex-5-enyl)-1*H*-pyrrole as the D subunit and *N*-(3,5-dihydroxyphenyl)indoline as the D' subunit, so that a broad absorption band and a low bandgap might be simultaneously acquired. Cheerfully, compared with those ASQ compounds we reported before, **Py-1** shows more widened absorption spectra in both solution and thin film states.^{7, 1c} In fact, in thin film state, **Py-1** displays an intense and broad absorption band in the Vis-NIR region of 550-950 nm with full width at half maxima (FWHM) of 232 nm (vide Fig. 1 and Table 1), which has effective overlap with the solar spectrum. In addition, the bandgap of **Py-1** is 1.37 eV, which falls into the ideal bandgap range (1.2-1.6 eV) for OPVs applications,⁹ and is lower than those of the OPV ASQ derivatives reported so far (≥ 1.43 eV).^{1c} However, **Py-1** shows rather poor solubility in common organic solvents (e.g., 7 mg/mL in chloroform), which might be ascribed to its rather planar molecular conformation hence severe π - π intermolecular stacking. Since the poor solubility of the opto-electronic materials should be disadvantageous to the fabrication of high-quality photoactive layers by spin-coating,¹⁰ bulk heterojunction (BHJ) SMOSC using **Py-1** as electron-donor and PC₇₁BM as electron-acceptor only exhibits a low PCE of 2.86% (device I, ITO/MoO₃ (8 nm)/**Py-1**:PC₇₁BM (1:5, 80 nm)/LiF (0.8 nm)/Al (100 nm); data shown in Table 2).

Consequently, to improve the processability of the objective compounds, we changed the 1-indolinyl D' subunit of **Py-1** into a cyclopenta[*b*]indolin-1-yl group bearing additional alkyl segments. As expected, the resulting compound **Py-2** (e.g., 20 mg/mL in chloroform) shows much enhanced solubility than **Py-1**;^{7b} and its bandgap is 1.37 eV, which is identical with that of **Py-1**. Further photophysical characterization results indicated that in dilute solution, the absorption spectrum of **Py-2** resembles that of **Py-1** (Fig. 1), implying that the alteration of indolin-1-yl into cyclopenta[*b*]indolin-1-yl would have little effect on the conjugation length of the resulting ASQs. While in solid film states, the FWHM of the absorption spectrum of **Py-2** is ~10 nm narrower than that of **Py-1**, suggesting that the presence of a less-coplanar cyclopenta[*b*]indolin-1-yl in **Py-2** would trigger alleviated intermolecular interactions.^{7b} Nevertheless, as intense molecular interactions in OPV materials would not only be propitious to the widening of the absorption spectra hence light-harvesting capability, but also be beneficial to the enhancement of charge-carrier mobility, to promote more effective intermolecular π - π stacking in these ASQs,¹¹ we designed and synthesized **Py-3**, in which an extra phenyl is fused onto the cyclopenta[*b*]indolin-1-yl segment of **Py-2**. Excitingly, **Py-3** not only shows good solubility in common organic solvents (e.g.,

Table 1. Optical, electrochemical and electric properties of **Py-1**~**3**.

Compd	λ_{abs}^a (nm)	λ_{abs}^b (nm)	FWHM (nm)		E_g^{opt} (eV)	E_{ox} (V)	HOMO ^c (eV)	LUMO ^d (eV)
	(log ϵ)		Solution	film				
Py-1	724(5.46)	770	50	232	1.37	0.29	-5.09	-3.72
Py-2	724(5.39)	770	50	222	1.37	0.29	-5.09	-3.72
Py-3	740(5.40)	784	61	227	1.33	0.29	-5.09	-3.76

^a Measured in dilute chloroform solution (2.00×10^{-6} M); ^b measured in thin film state; ^c derived from CV measurement results, HOMO = $(-4.80 - E_{\text{ox}})$ eV; ^d LUMO = $E_g^{\text{opt}} + \text{HOMO}$.

16 mg/mL in chloroform), but also displays ~15 nm red-shifted λ_{abs} than **Py-2** in both solution and solid-film states. In fact, in comparison with **Py-2**, **Py-3** displays an even lower bandgap of 1.33 eV and a ~5 nm larger FWHM in its absorption spectrum in solid film state. Therefore, the presence of benzo[*e*]cyclopenta[*b*]indolin-1-yl D' group in **Py-3** could endow it with not only more extended conjugation length hence lower bandgap, but also stronger intermolecular interactions hence broadened absorption band. Moreover, all the three objective compounds **Py-1**~**3** exhibit considerably high molar extinction coefficients of $\sim 10^5$ L mol⁻¹ cm⁻¹. Taking into account that **Py-3** has strong and broad absorption in the Vis-NIR region together with low bandgap of 1.33 eV, it should be a more perspective candidate in SMOSC applications.

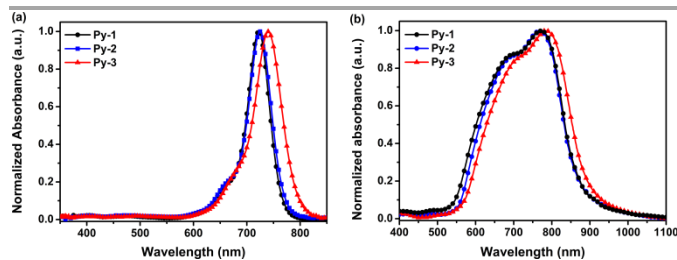


Fig. 1 Absorption spectra of molecules in solution (a) and thin films (b).

Additional cyclic voltammetry (CV) measurements indicated that all these three compounds show two-electron reversible oxidation wave at 0.29 V and 0.69 V during the anodic scan, hence the highest occupied molecular orbital (HOMO) energy levels of **Py-1**~**3** were all calculated to be -5.09 eV. While the lowest unoccupied molecular orbital (LUMO) energy levels of **Py-1**, **Py-2** and **Py-3** were estimated to be -3.72 eV, -3.72 eV and -3.76 eV in sequence according to the HOMO energy level and optical bandgap data (Table 1 and Fig. S1 in the ESI[†]).

To gain deeper insight into the relationship between molecular structure and photovoltaic properties of these objective ASQ compounds, two solution-processed BHJ SMOSCs with similar device structure of **Py-1**-based device I were fabricated using **Py-2** (device II) and **Py-3** (device III) as the electron donor, respectively. The representative photovoltaic data of these devices are summarized in Table 2, and the current density-voltage (*J*-*V*) and external quantum efficiency-wavelength (EQE) curves are shown in Fig. 2. In comparison with device II, device III shows analogous V_{oc} but higher J_{sc} (11.22 mA cm⁻² vs 10.32 mA cm⁻²) and higher FF (0.46 vs 0.42), hence higher PCE (3.98% vs 3.30%). In principle, J_{sc} should correlates highly not only with the light-harvesting capability and the hole-mobility of the electron-donor materials, but also with the morphology of the donor-acceptor blending films,¹² hence we firstly investigated the EQE curves of devices II and III. As shown in Fig. 2b, consistent with the absorption spectral properties of **Py-2** and **Py-3** in thin film state, more broadened spectral response toward EQE could be observed in device III than device II. The integration areas of the EQE curves in 300-900 nm were calculated to be 159.5 for device II and 175.4 for device III, implying that the more

Table 2 Photovoltaic performance of BHJ-OPVs based on **Py-1-3**.

Device	Active layer (w/w)	V_{oc} (V)	J_{sc} (mA cm ⁻²)	FF	PCE (%)
I	Py-1:PC ₇₁ BM=1:5	0.75±0.01	9.40±0.17	0.39±0.02	2.81±0.05
II	Py-2:PC ₇₁ BM=1:5	0.78±0.01	10.08±0.24	0.40±0.02	3.16±0.14
III	Py-3:PC ₇₁ BM=1:5	0.78±0.01	10.98±0.24	0.44±0.02	3.75±0.23
IV	Py-2:PC ₇₁ BM=1:5 ^a	0.79±0.01	10.82±0.22	0.42±0.02	3.58±0.14
V	Py-3:PC ₇₁ BM=1:5 ^a	0.78±0.01	11.80±0.23	0.45±0.02	4.12±0.23

^a Device annealed at 70 °C for 10 min.

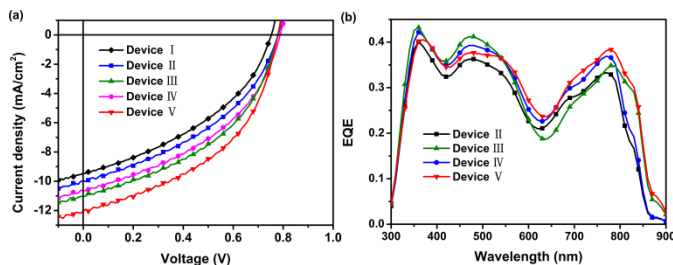


Fig. 2 J - V characteristics (a) and EQE characteristics (b) of the OPV devices.

broadened absorption band of **Py-3** relative to **Py-2** indeed contributes to the light-harvesting hence the enhancement of J_{sc} in device III than device II. Subsequently, we measured the hole-mobility of the neat ASQ films and ASQ/PC₇₁BM blended ones by a space charge limited current (SCLC) method. According to the experimental and calculation results, the hole-mobility of the **Py-2** and **Py-3** films is 5.21×10^{-5} cm² V s⁻¹ and 5.56×10^{-5} cm² V s⁻¹, respectively; and that of the **Py-2**/PC₇₁BM and **Py-3**/PC₇₁BM composite film is 3.27×10^{-6} cm² V s⁻¹ and 4.95×10^{-6} cm² V s⁻¹, respectively (Fig. S2, ESI[†]). Obviously, **Py-3** shows higher hole-mobility than **Py-2** in both neat and ASQ/PC₇₁BM composite films, which may be attributed to the more effective intermolecular packing triggered by its benzo[e]cyclopenta[b]indolin-1-yl D' segment with more extended π -system.¹¹ Further AFM characterization results revealed that both the **Py-2**/PC₇₁BM and **Py-3**/PC₇₁BM composite films show quite smooth surfaces with analogous root-mean-square (RMS) of 0.25 nm and 0.23 nm, respectively (Fig. S3, ESI[†]). Consequently, the higher J_{sc} of device III relative to device II should originate from the broadened absorption band and higher hole-mobility of **Py-3** relative to **Py-2**. In addition, the FF of device III is higher than that of device II (0.46 vs. 0.42), which might also arise from the higher hole-mobility of **Py-2**.¹³

Because thermal annealing is a well-adopted process for enhancing the performance of OPV devices,¹⁴ device IV (**Py-2**-based) and device V (**Py-3**-based) with their photoactive layers annealed at 70 °C for 10 min were fabricated. As shown in Fig. 2 and Table 2, upon thermal treating, the PCEs of both devices IV (3.72%) and V (4.35%) were increased relative to device II and III, respectively. It is noteworthy that, to the best of our knowledge, the J_{sc} of 12.03 mA cm⁻² and the PCE of 4.35% in device V are both the record ones in ASQ-based OPV devices.^{1e, 2a} In fact, the OPV devices reported here have not been further optimized, and more improved device performance could be expected if additional optimizations on blending ratio of the electron-donor/electron-acceptor, solvent-annealing and additives have been carried out.

In summary, a series of novel ASQ derivatives **Py-1-3** were designed and synthesized. Different from those known high performance OPV ASQs whose D aryls are generally directly connected to the A subunit but D' aryls are linked to the A subunit via a methylylidene bridge, **Py-1-3** have both their D and D' aryls linked directly to the A subunit. Through rational molecular design, **Py-3** showing good solubility, relative low bandgap, broad and intense absorption band in Vis-NIR region, and effective

intermolecular packing property has been achieved. BHJ-SMOSCs using **Py-3** as electron-donor material show high photovoltaic performance with PCE of 4.35% and J_{sc} of 12.03 mA cm⁻², both are the highest values among BHJ-SMOPVs with ASQs as electron-donor materials. All these preliminary results indicated that ASQ derivatives with their D and D' aryls linked to the A subunit directly should be quite promising OPV electron-donor materials.

We acknowledge the financial support for this work from the National Natural Science Foundation of China (project No.21432005, 21190031 and 21372168) and the Research Fund for the Doctoral Program of Higher Education (No.20120009130005). We also thank the Analytical & Testing Center, SCU, and Comprehensive Training Platform of Specialized Laboratory, College of Chemistry, SCU for providing NMR and HRMS data for the intermediates and objective molecules.

Notes and references

- (a) D. Bagnis, L. Beverina, H. Huang, F. Silvestri, Y. Yao, H. Yan, G. A. Pagani, T. J. Marks and A. Facchetti, *J. Am. Chem. Soc.*, 2010, **132**, 407; (b) F. Silvestri, M. D. Irwin, L. Beverina, A. Facchetti, G. A. Pagani and T. J. Marks, *J. Am. Chem. Soc.*, 2008, **130**, 17640; (c) G. Chen, H. Sasabe, Y. Sasaki, H. Katagiri, X. Wang, T. Sano, Z. Hong, Y. Yang, and J. Kido, *Chem. Mater.*, 2014, **26**, 1356; (d) L. Beverina, and P. Salice, *Eur. J. Org. Chem.*, 2010, 1207; (e) D. Yang, Q. Yang, L. Yang, Q. Luo, Y. Chen, Y. Zhu, Y. Huang, Z. Lu and S. Zhao, *Chem. Commun.*, 2014, **50**, 9346; (f) S. L. Lam, X. Liu, F. Zhao, C. L. Lee and W. L. Kwan, *Chem. Commun.*, 2013, **49**, 4543.
- (a) B. A. Rao, K. Yesudas, G. S. Kumar, K. Bhanuprakash, V. J. Rao, G. D. Sharama and S. P. Singh, *Photochem. Photobiol. Sci.*, 2013, **12**, 1688. (b) U. Mayerhoffer, K. Deing, K. Gruss, H. Braunschweig, K. Meerholz and F. Würthner, *Angew. Chem. Int. Ed.*, 2010, **132**, 4074; (c) I. A. Karpenko, A. S. Klymchenko, S. Gioria, R. Kreder, I. Shulov, P. Villa, Y. M'ay, M. Hibert and D. Bonnet, *Chem. Commun.*, 2015, **51**, 2960.
- S. Sreejith, P. Carol, P. Chithras and A. Ajayaghosh, *J. Mater. Chem.*, 2008, **18**, 264.
- L. Beverina, R. Ruffo, G. Patriarca, F. De Angelis; D. Roberto, S. Righetto, R. Ugo and G. A. Pagani, *J. Mater. Chem.*, 2009, **19**, 8190.
- G. Wei, S. Wang, K. Sun, M. E. Thompson and S. R. Forrest, *Adv. Energy Mater.*, 2011, **1**, 184.
- (a) S. So, H. Choi, H. M. Ko, C. Kim, S. Paek, N. Cho, K. Song, J. K. Lee and J. Ko, *Sol. Energy Mater. Sol. Cells*, 2012, **98**, 224; (b) K. C. Deing, U. Mayerhoffer, F. Würthner and K. Meerholz, *Phys. Chem. Chem. Phys.*, 2012, **14**, 8328.
- (a) D. Yang, Q. Yang, L. Yang, Q. Luo, Y. Huang, Z. Lu and S. Zhao, *Chem. Commun.*, 2013, **49**, 10465; (b) L. Yang, Q. Yang, D. Yang, Q. Luo, Y. Zhu, Y. Huang, S. Zhao and Z. Lu, *J. Mater. Chem. A*, 2014, **2**, 18313.
- C. Gude and W. Retting, *J. Phys. Chem. A*, 2000, **104**, 8050.
- X. Liu, Y. Sun, B. B. Y. Hsu, A. Lorbach, L. Qi, A. J. Heeger and G. C. Bazan, *J. Am. Chem. Soc.*, 2014, **136**, 5697.
- (a) B. Walker, C. Kim and T.-Q. Nguyen, *Chem. Mater.*, 2011, **23**, 470; (b) S. Wang, L. Hall, V. V. Diev, R. Haiges, G. Wei, X. Xiao, P. I. Djurovich, S. R. Forrest and M. E. Thompson, *Chem. Mater.*, 2011, **23**, 4789.
- (a) S. Paek, N. Cho, S. Cho, J. K. Lee and J. Ko, *Org. Lett.*, 2012, **14**, 6326; (b) O. P. Lee, A. T. Yiu, P. M. Beaujuge, C. H. Woo, T. W. Holcombe, J. E. Millstone, J. D. Douglas, M. S. Chen and J. M. J. Fréchet, *Adv. Mater.*, 2011, **23**, 5359.
- B. Kan, Q. Zhang, M. Li, X. Wan, W. Ni, G. Long, Y. Wang, X. Yang, H. Feng and Y. Chen, *J. Am. Chem. Soc.*, 2014, **136**, 15529;
- J. Zhou, Y. Zou, X. Wan, G. Long, Q. Zhang, W. Ni, Y. Liu, Z. Li, G. He, C. Li, B. Kan, M. Li and Y. Chen, *J. Am. Chem. Soc.*, 2013, **135**, 8484.
- Y. Huang, E. J. Kramer, A. J. Heeger and G. C. Bazan, *Chem. Rev.*, 2014, **114**, 7006.